Prediction of Straight Tooth Milling of Scots Pine Wood by Shank Cutter Based on Neural Net Computations and Regression Analysis

Jiali Gu and Pingxiang Cao *

Regression models and a neural net approach were used to predict the cutting performance during milling of Scots pine (*Pinus sylvestris* L.) by shank cutter. The influence of rake angle, spindle speed, and milling depth on surface roughness of the workpiece, as well as the connection between the milling force and the surface roughness, were thoroughly considered. Four approaches were used to predict the workpiece's surface roughness based on the experimental data: Back Propagation Neural Network (BPNN), Radial Basis Function Neural Network (RBFNN), Support Vector Machines (SVM), and multiple linear regression. The comparative analysis of the predictive models showed that Neural Network (NN) had preferable performance for prediction of machined surface roughness, with an R^2 of 0.98. The SVM had certain fluctuations and the R^2 of the multiple linear regression was just 0.87, indicating that they did not fit well for prediction machined surface roughness. In summary, the effective trend of milling parameters on the machined surface roughness of Scots pine was similar to multiple nonlinear regression, and the accurate prediction by BPNN model can provide technical support for the surface roughness of the Scots Pine and enhance shank cutter performance.

DOI: 10.15376/biores.17.2.2003-2019

Keywords: Scots pine; Straight tooth milling; Surface roughness; NN; SVM; Multiple linear regression

*Contact information: College of Materials Science and Engineering, Nanjing Forestry University, 210037, Jiangsu, China; *Corresponding author: njfucpx@163.com*

INTRODUCTION

Scots pine is a type of softwood that grows in many places of the world. It usually has a light yellowish color and a broad texture pattern (Zhong *et al.* 2013). It also has low processing energy consumption, natural degradation, and suitability for recycling (Tu *et al.* 2018). As a typical material with heterogeneity and anisotropy, Scots pine is distinctive relative to other wood species (Eyma *et al.* 2004). The properties and strength vary in different directions (Guo *et al.* 2021). In the field of wood cutting mode, milling is one of the most widely used cutting methods. The spindle speed of the milling cutter is generally above 3000 r/min and up to 24000 r/min (Zheng *et al.* 2008). High-speed milling enables wood processing with high productivity and smooth surface quality (Darmawan *et al.* 2001; Byrne *et al.* 2003; Guo *et al.* 2021).

The selection of milling cutters mainly includes the technical parameters (Vančo *et al.* 2017), the structure (Keturakis and Bendikiene 2016), the direction of rotation (Chen *et al.* 2012), the cutting amount (Luo 2007), and the stable operation of the milling cutter (Sofuoğlu 2019). The shank cutter is a type of milling cutter that has a small diameter with high rotational speed to reach high productivity (Guo *et al*. 2014).

In wood manufacturing, the surface roughness significantly impacts the sealing performance (Liu *et al.* 2018), painting (Zhang *et al.* 2015), surface decoration quality (Sogutlu *et al.* 2017), adhesive usage (Rudawska *et al.* 2016), and paint consumption (Zhu *et al.* 2018), so it is an important index to evaluate the surface quality of wood products. Moreover, the surface roughness of wooden parts was found to directly affect the arrangement of the processing technology and the setting of the processing allowance. Guo *et al.* (2015) studied the wood floor/PVC machinability of composite material. These authors concluded that the roughness of the machined surface increased as the depth of milling increased. MalkoçOğLu (2007) measured the surface roughness of Scots pine and indicated that the rake angle affected the surface roughness of the wood, and the effect of the feed speed on the surface roughness was negligible.

As technology advances, the emergence of some mathematical models also provides reference and contrast for physical experimental analysis. In the existing analysis technology of the cutting performance of wood products, Tiryaki *et al.* (2014) used artificial neural networks to model the type of wood, the number of cuts, the feed speed, the depth of cut, and the early and fall wood. The conclusion was that the model of wood surface roughness was reliable and valuable. Dong *et al.* (2021) proposed a tool wear status monitoring method based on wavelet transform and genetic-BP neural network. Valarmathi *et al.* (2015) used response surface methodology to establish a mathematical model that predicted the influence of input control parameters on the cutting force generated during the medium density fiberboard (MDF) drilling. Yue *et al.* (2017) developed serials of 3D FEM models for the corner milling process based on DEFORM software. Tool curved trajectory was achieved by tool location with milling time, and the results provided a guide for optimizing cutting parameters in the cutting process. Analysis of variance was used to test the adequacy of the model. Although there have been some successes in predicting automation for analyzing wood cutting performance, the accuracy of predicting these parameters used to evaluate cutting performance needs to be improved and the prediction of surface roughness needs to be studied, which will serve as a reference for improving wood quality.

In this paper, multiple milling parameters were used to explore the machined surface quality of Scots pine by shank cutter with a single tooth. The effects of rake angle, spindle speed, and milling depth on the surface roughness of the workpiece, as well as the connection between the milling force and the surface roughness, were thoroughly analyzed. Based on the experimental data, four different computational approaches were utilized to predict the workpiece's surface roughness. The performances of the four approaches were compared and examined in order to provide a reliable prediction model for Scots pine straight-tooth milling.

EXPERIMENTAL

Materials

The milling experiments were carried out on a computerized numerical control (CNC) processing center (MGK01, Nanxing Machinery Co., Ltd., Guangzhou, China) with an 18 mm diameter shank cutter. The shank cutter (Fig. 1) in the milling process with a single tooth which was made of cemented carbide. The angle geometries and mechanical properties are shown in Table 1. The tool rake angles of 2°, 6°, and 10° were selected in the experiments because the smaller rake angle provided stable milling force and made the

tool more durable. The workpiece was made from Scots pine. The size was 120×80×12 (length×width×thickness) mm, and the feed speed during machining was fixed at 5 m/min.

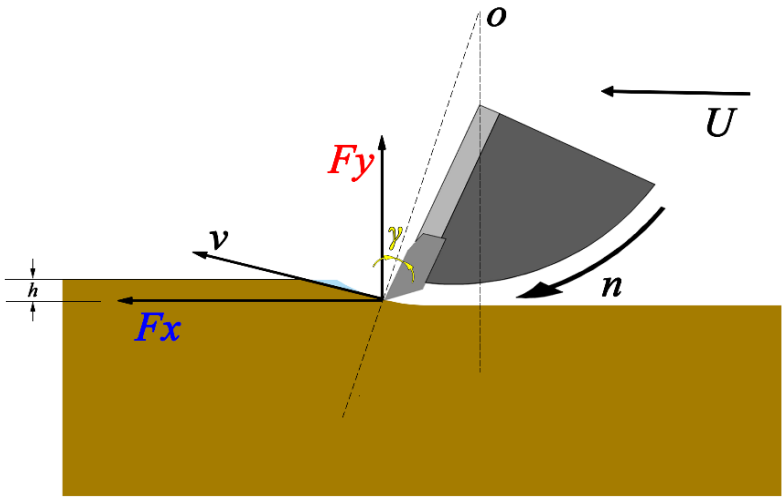

Fig. 1. Cutting diagram

Table 1. Rake Angles and Mechanical Properties of Shank Cutter Tooth

Blades	Rake Angle (°)			Mechanical Properties			
Cemented carbide	2°	6°	10°	Bending strength (GPa)	Thermal conductivity (W/(m·K))	Hardness (HRA)	Density (g/cm^3)
				1.48	75.36	88	14.7

Experimental Design

The milling force F_x is parallel to feed rate U, and F_y is perpendicular to the direction of feed rate U. The milling forces were measured by Kistler dynamometer (9257B, Kistler Group, Winterthur, Switzerland) equipped with a sensor and a charge amplifier. In the straight tooth milling process, the workpiece would be fixed by the fixture in actual production. The F_z component of force was weak and was assumed not have an influence on milling performance, and it was not considered. The software of Dynoware (Kistler 5070A amplifier, 3.2.0.0, Kistler Group, Winterthur, Switzerland) was used to measure the milling force in the process. Each milling parameters will be performed eight times, and the measured F_x and F_y values were selected from last five times out of eight times and calculated as the absolute maximum of each time. The milling parameters selected in the experiment are shown in Table 2.

Table 2. Factor Levels Assignment

Factor	Unit	Notation	Factor Levels		
			Level 1	Level 2	Level 3
Rack angle	°	γ	2	6	10
Spindle speed	r/min	n	6000	8000	10000
Milling depth	mm	h	0.5	1	1.5

The horizontal tracking surface roughness of the machined workpiece was measured by a precision surface roughness profiler (SURFCOM NEX, Zeiss, Oberkochen, Germany) with a probe head. The surface roughness under each group of milling parameters was measured five times. The data for R_a were the averages calculated after removing the maximum and minimum values five times.

In the experiment, 27 groups of data under 3 milling parameters were conducted. Rake angle, spindle speed, and milling depth were the independent variables. The milling force in two directions and the surface roughness were the dependent variables. The surface roughness was a significant signal for evaluating the surface quality of Scots pine, and the resultant milling force function was as stated in Eq. 1.

$$F_c = \left(F_x^2 + F_y^2\right)^{1/2} \quad (1)$$

RESULTS AND DISCUSSION

Effect of Rake Angle on Surface Roughness

In the milling process, the tool rake angle had a significant influence on the machined surface roughness. Individual value graphs of surface roughness *vs.* rake angle are shown in Fig. 2. The workpiece surface roughness decreased when the rake angle was raised. The reason for this was that the shank cutter's extrusion and friction on the chip's front face were reduced, resulting in less chip plastic deformation. As a result, the stiffness damage on the machined surface decreased, and the surface quality increased.

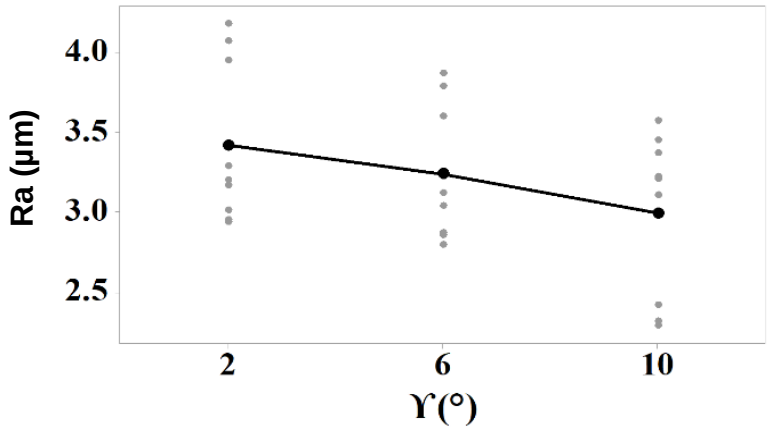

Fig. 2. Effects of rake angle on the surface roughness of workpiece

Effect of Spindle Speed on Surface Roughness

The effects of workpiece surface roughness with different spindle speeds are shown in Fig. 3. The rake angles of 2°, 6°, and 10° are indicated in the three columns from left to right. The results revealed that when the spindle speed increased, the surface roughness of the machined workpiece was reduced. The reason was that when the spindle speed increased, the average milling amount reduced. The impulsive load was lowered, which had an additional impact on the blade load and vibration. More crucially, within a given range (6000 to 10000 r/min), the spindle speed was the key factor of three (rake angle, spindle speed and milling depth) related to variations in surface roughness. As a result,

increasing the spindle speed enhanced the quality of the machined surface dramatically. However, with the same machining allowance, it would increase the number of milling rotations, causing the wear of milling edges to accelerate.

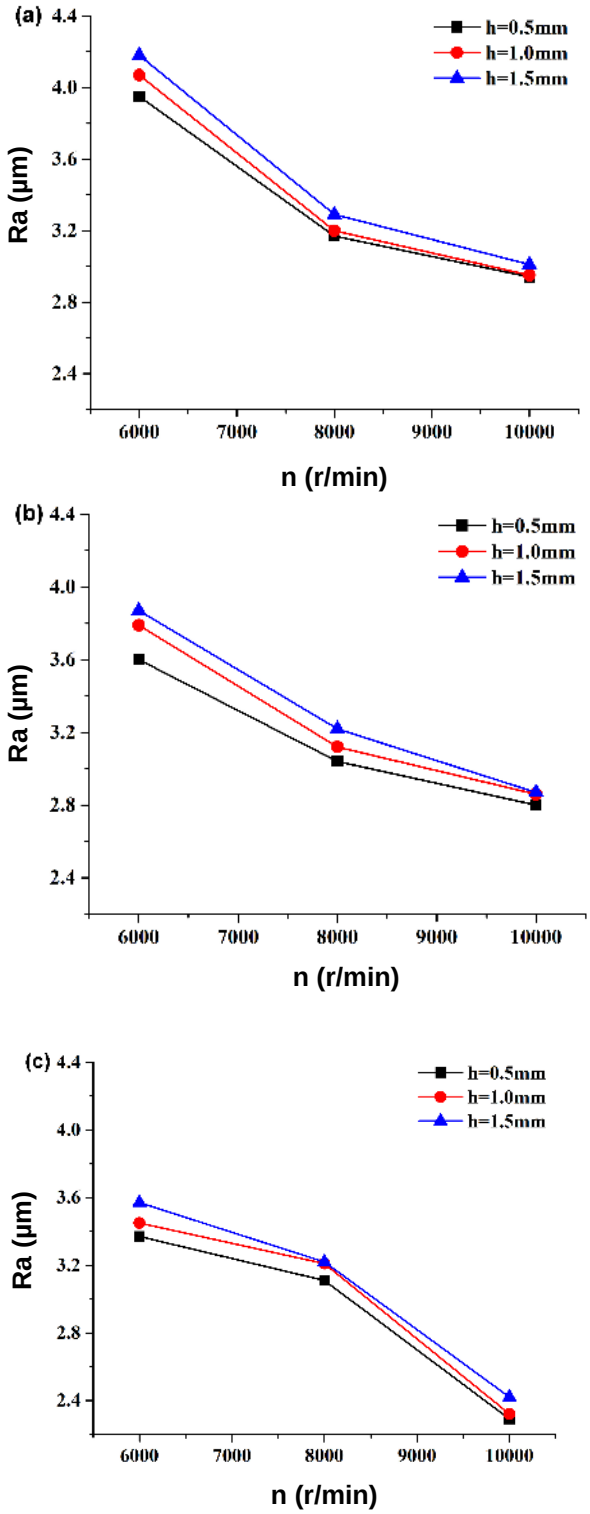

Fig. 3. Effects of spindle speed on the surface roughness of workpiece: (a) γ = 2°, (b) γ = 6°, and (c) γ = 10°

Effect of Milling Depth on Surface Roughness

The milling depth also had an influence on the surface roughness of the workpiece while milling with a shank cutter. The machined surface roughness increased with the average milling depth when the tool angle was constant, as illustrated in Fig. 4. The primary reason was that the quantity of milling per tooth increased, as did the length and thickness of the chips.

It should be noted that when the spindle speed was set to 10000 r/min, the roughness changes with increasing milling depth were not obvious. This was mostly due to the high temperature in the milling zone at this speed (Umut and Erhan 2018), which exacerbated the workpiece's softening impact. As a result, if high-speed milling was used and the workpiece's surface quality met the criteria, the production efficiency could be enhanced by increasing the milling depth. However, it could not be increased arbitrarily, which would result in decreased tool life.

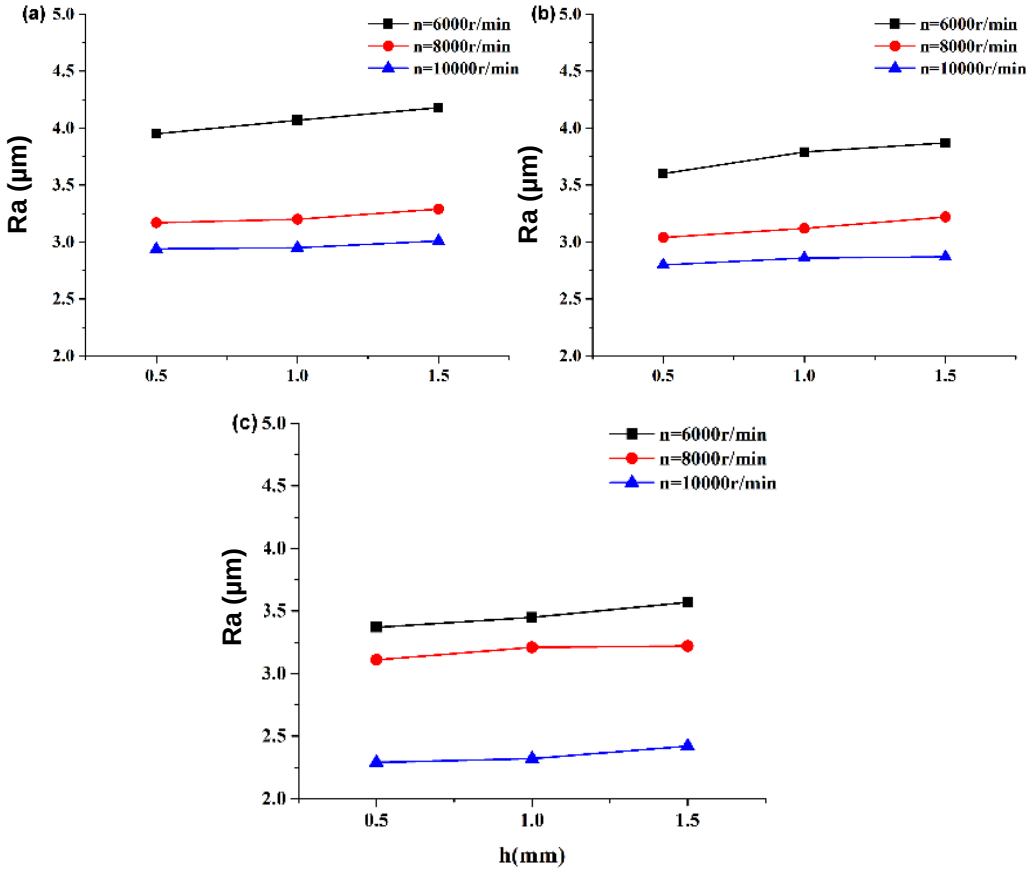

Fig. 4. Effects of milling depth on the surface roughness of workpiece: (a) γ = 2°, (b) γ = 6°, and (c) γ = 10°

Relationship between Milling Force and Surface Roughness

According to the above analysis, it was concluded that the fluctuation range of the spindle speed had a greater effect on the workpiece surface roughness than the other two parameters. Figure 5 displays the changing trend between the resultant milling force F_c and surface roughness R_a under the conditions that when γ = 2°, 6°, 10° and h = 0.5 mm, 1 mm and 1.5 mm. It was concluded that the resultant milling force had a good correlation with the surface roughness. They both decreased when the spindle speed was increased. As a

result, the workpiece's surface quality improved. It was mainly because the rake face of the shank cutter made it simpler to separate the chips from the milling surface of the workpiece as the spindle speed increased. The surface groove markings were trimmed back and the friction between the rake face and the workpiece was minimized.

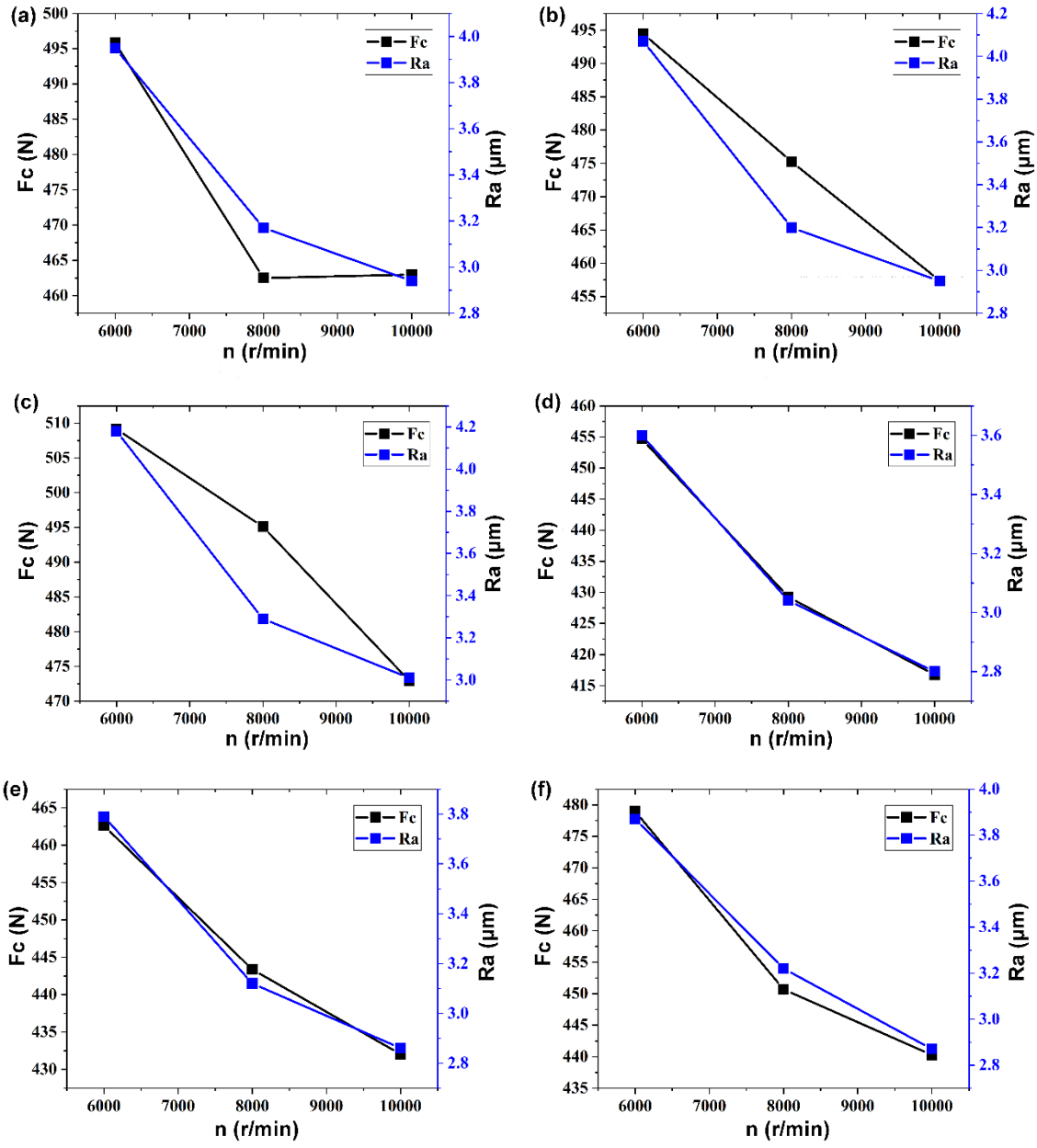

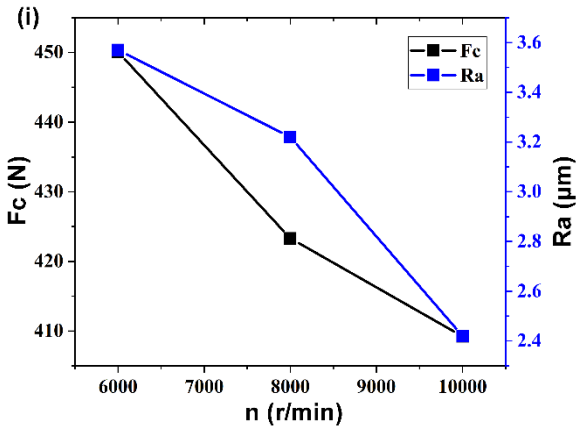

Fig. 5. Relationship between the resultant milling force and surface roughness: (a) γ = 2°, h = 0.5 mm, (b) γ = 2°, h=1 mm, (c) γ = 2°, h = 1.5 mm, (d) γ = 2°, h = 0.5 mm, (e) γ = 6°, h = 1 mm, (f) γ = 10°, h = 1.5 mm, (g) γ = 2°, h = 0.5 mm, (h) γ = 6°, h = 1 mm, and (i) γ = 10°, h = 1.5 mm

PREDICTION AND VALIDATION OF COMPUTATIONS

Data Pre-processing

Due to the complexity and random nature in the milling process of Scots pine with shank cutter, methods of achieving suitable surface roughness should be involved in the prediction. Regression models have been extensively applied in the field of wood processing because of their ability to extract features from complicated factors and detect patterns.

The data pre-processing was necessary for prediction of regression models and for neural net computations. The machining variables (including the rake angle, spindle speed, and milling depth) were measured in different units and dimensions, which influenced the data analysis findings. As a result, the normalization procedure should be carried out between the variables in order to increase the stability and performance of regression models (Liu *et al.* 2020). Equation 2 depicts the normalizing procedure,

$$y = \frac{x - x_{\min}}{x_{\max} - x_{\min}} \quad (2)$$

where x is the input value of the sample, and $x_{\min}$ and $x_{\max}$ are the sample's minimum and maximum values, respectively.

Modeling of Surface Roughness Based on Milling Parameters

Nonlinear and linear regression models were included in the computational approaches. Nonlinear computational approaches with properties of optimum and global approximation, such as back propagation neural network (BPNN), radial basis function neural network (RBFNN), and support vector machines (SVM), have been frequently used to predict milling processes. Multiple and univariate linear regression were used in the linear regression models. Three types of computational approaches (NN, SVM, and multiple linear regression) were employed to predict surface roughness during the milling of Scots Pine with a shank cutter in this paper. In addition, the accuracy of nonlinear and linear regression was also compared.

BPNN Modeling

The BPNN is a multilayer feed-forward network that uses the error back propagation method to cope with nonlinear and complicated systems (Zhang *et al.* 2018). The BPNN adopts the Sigmoid function for the global approximation of nonlinear mapping (Cui and Xiang 2018). The structure of BPNN in this paper is shown in Fig. 6, and the Sigmoid function can be formulated as Eq. 3,

$$f(z) = \frac{1}{1+e^{-z}} \tag{3}$$

where $f(z)$ represents an activation function for the output of the hidden layer, and z is sum of the multiplication of the input value and the weights.

Forward propagation

The forward propagation of the signal means that the input samples are transmitted from the input layer, processed one by one by each hidden layer, and then transmitted to the output layer (Wang and Chen 2005). The transfer function of the hidden layer is $f_1(\cdot)$, and the transfer function of the output layer is $f_2(\cdot)$; then the output of the hidden and output layer is given as Eqs. 4 and 5 (Ma *et al.* 2016).

$$z_k = f_1\left(\sum_{i=0}^{n} v_{ki} x_i\right) \quad k=1,2, \ldots, q \tag{4}$$

$$y_j = f_2\left(\sum_{k=0}^{q} w_{jk} z_k\right) \quad j=1, 2, \ldots, m \tag{5}$$

where v_{ki} is the weight between the input and the hidden layer, x_i is the weight between the hidden and output layer, z_k is the output of the hidden layer node, and y_j is the output of the output layer.

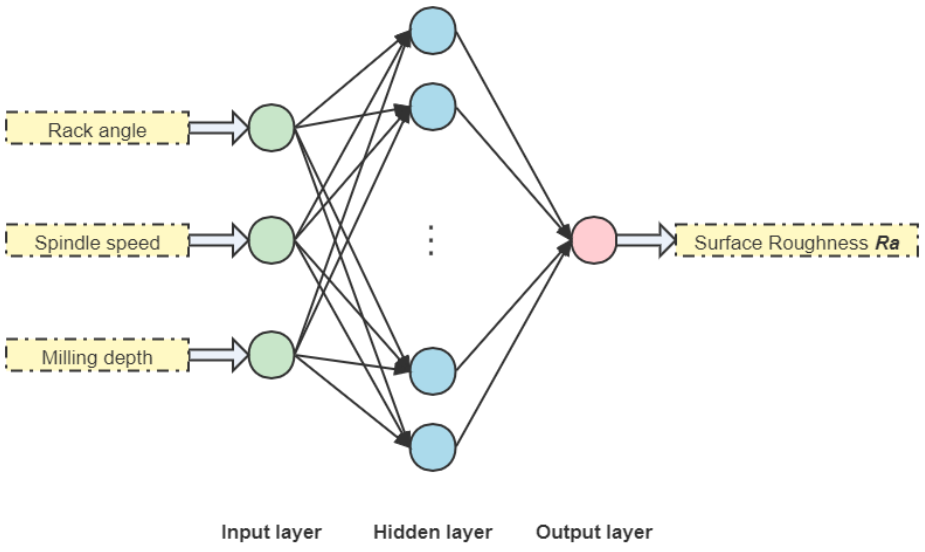

Fig. 6. Topological structure of three-layer BPNN

Back propagation

The back propagation of errors means that the output is transmitted back to the input layer through the hidden layer. The error is allocated to all neural units in each layer, allowing the weights of each layer's neural units to be adjusted to reduce the error along the gradient (Zhao *et al.* 2008).

RBFNN Modeling

In common with BPNN, the RBFNN is also a typical nonlinear multilayer feedforward NN. The distinction is that RBFNN adopts radial basis functions (such as Gaussian function) for the local nonlinear mapping approximation (Sun *et al.* 2019). Therefore, the RBFNN has the characteristics of fast learning speed and strong adaptability. The construction of RBFNN in this paper was comparable to that of BPNN, as showed in Fig. 6.

In RBFNN, the output of the hidden and output layer is given in Eqs. 6 and 7.

$$b_j(x) = \exp\left(-\frac{\left\|x - c_j\right\|^2}{2\sigma_j^2}\right),\ j = 1, 2, \cdots, p \tag{6}$$

$$y_i = \sum_{j=1}^{m} w_{ij} b_j(x), i = 1, 2, \cdots, m \tag{7}$$

where c_j is the center value of Gaussian function, x is the input value of the sample, σ_j represents extension constant or width, and w_{ij} is the weight from hidden layer to the output layer.

The graph of the RBFNN function is radially symmetric and decaying on both sides. When the specified center is relatively near to the input data, the mapping on the input works. On the other hand, if the center is far away from the input data, the output of result tends to zero, making it a local approximation (Guillén *et al.* 2009).

SVM Modeling

Compared with NN, the SVM does not have hidden layer and neurons. The SVM conducts classification by creating an N-dimensional hyperplane that divides the input into two groups as efficiently as possible (Cho *et al.* 2005). The SVM adopts a kernel function to perform nonlinear mapping to high-dimensional space (Li *et al.* 2013), so it is well-suited to problems that are fundamentally nonlinear, such as classification, regression, and density function estimation.

Given the mapping to high-dimensional space, the model corresponding to dividing the hyperplane in this feature space is expressed in Eq. 8,

$$f(x) = \omega^T \phi(x) + b \tag{8}$$

where w^T and b are the weight vector and bias term, respectively, and $\Phi(x)$ is the mapping from the input space to the feature space.

In the dual problem of SVM learning, both the objective function and the classified decision function only include the inner product of the instances; hence, the kernel function is used instead and stated in Eq. 9.

$$K(x, z) = \phi(x) \cdot \phi(z) \tag{9}$$

In Eq. 9, x and z are input value of the sample, whereas $\phi(x)$ and $\phi(z)$ represent the mapping from the input space to the feature space.

Finally, the nonlinear SVM are solved which can be formulated as Eq. 10,

$$f(x) = sign(\sum_{i=1}^{N} \alpha_i^* y_i K(x, x_i) + b^*) \quad (10)$$

where α_i^* ($0 < \alpha_i^* < C$, C represents penalty parameter) is one component of the Lagrange multiplier vector, y_i ($y_i \epsilon \{-1, +1\}$) is the type of mark, b^* is bias term vector.

Multiple Linear Regression Modeling

To comprehensively consider the unknown function model about the impacts of milling parameters on surface roughness, it is necessary to perform multiple linear regression analysis on it.

The model of multiple linear regression can be formulated as Eq. 11 (Wang *et al.* 2006),

$$Y = b_0 + b_1 x_1 + b_2 x_2 + \cdots + b_i x_i \quad (11)$$

where Y is the observation of the dependent variables, x_i represents the ith input value of the sample, and b_0 and b_i represent regression coefficients.

Comparison of Different Predictive Methods

In the process of prediction, the proposed NN had 3 input variables (rake angle, spindle speed, milling depth) and 1 output variable (surface roughness), as shown in Fig. 6. In addition, the number of neurons and iterations in the hidden layer that were chosen had varying degrees of impact on the training outcomes. 22 of 27 datasets were randomly selected for training to be conducted by Matlab 2017a.

For the BPNN computations, the parameters were set through training as follows: the number of neurons and iterations were 7 and 6000, respectively. The learning rate was 0.01. For the RBFNN computations, the spread parameter of prediction was set to 30. For the multiple linear regression model, the regression coefficients of b_0, b_1, b_2, b_3 obtained after fitting was 0.8489, -0.2324, -0.5650 and 0.0791 under the condition that input variables were the normalized values.

The predictive results of the surface roughness by the four computational approaches (BPNN, RBFNN, SVM, and multiple linear regression) and the 5 training datasets are showed in Fig. 7. The predicted values were demonstrated to have a good correlation with the experimental values. Furthermore, to quantify the predictive accuracy between 4 models, the mean absolute percentage (MAP) was employed as Eq. 12,

$$MAP = \frac{1}{n} \sum_j \left| \frac{t_j - y_j}{y_j} \right| \times 100\% \quad (12)$$

where n is the number of training samples, and t_j and y_j indicate the ith predictive output and experimental output.

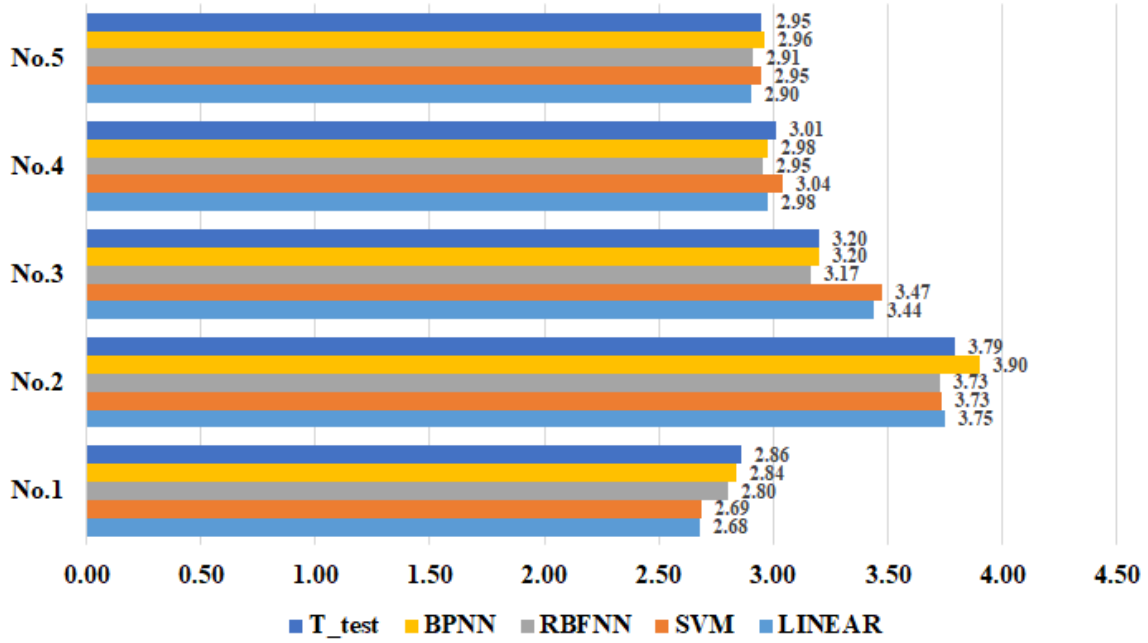

Fig. 7. The predictive results of surface roughness by the models

Table 3. Evaluation Criteria for Predictive Results of Models

Regression Model	MAP	MSE	R^2
BPNN	1.02%	0.0114	0.98
RBFNN	1.60%	0.0143	0.98
SVM	3.39%	0.0167	0.95
LINEAR	3.48%	0.0231	0.87

Table 3 shows that the MAP of the 5 groups was kept to less than 4%, and the BPNN model was relatively minimal. Additionally, SVM and multiple linear regression errors were more than twice as large as NN's. The experimental surface roughness of No.1 was 2.86 µm, and the SVM and multiple linear regression prediction values were 2.69 µm and 2.68 µm, respectively, as shown in Fig. 7. The data discrepancy between experimental and predicted surface roughness of SVM, multiple linear regression is similarly considerable in the No. 3 group. As a result, the inaccuracy of prediction was caused by the two groups. Based on the relative errors, the construction of the NN was more accurate and effective for the fitting analysis of the surface roughness model than other two models.

Furthermore, in analysis of peformance among 4 models, the mean square error (MSE) and goodness of fit (R^2) were used as evaluation criteria. The MSE reflected the degree of difference between the predictive value and exprimental value and could be expressed as Eq. 13,

$$MSE = \frac{1}{\mathrm{mp}} \sum_{p=1}^{P} \sum_{j=1}^{m} (\hat{y}_{pj} - y_{pj})^2 \quad (13)$$

where m is the number of output nodes, p is the number of training samples, and $\hat{y}_{pj}$ and y_{pj} are the predictive output and experimental output, respectively.

The R^2 described how well it fit a set of observations. The maximum value of R^2 was 1. The closer the value of R^2 was to 1, the better the fit of the regression to the tested

values. On the contrary, the smaller the value of R^2, the worse the fit of the regression to the tested values. For multiple nonlinear regression and multiple linear regression, the R^2 was expressed as Eqs. 14 and 15 (Gharagheizi 2007), respectively.

$$R^2 = 1 - \sqrt{\frac{\sum_{i=1}^{k}(y_i - y_i^*)^2}{\sum_{i=1}^{k} y_i^2}} \quad (14)$$

$$R^2 = 1 - \frac{\sum_{i=1}^{k}(y_i - y_i^*)^2}{\sum_{i=1}^{k}(y_i - \bar{y}_i)^2} \quad (15)$$

In these equations, y_i and y_i^* are the experimental and predictive output, and $\bar{y}_i$ is the average of experimental output.

According to the results of MSE and R^2 in Table 4, it should be noted that the performance result of NN was perfect among the four computational approaches, with the R^2 of 0.98. In particular, the fitting process of BPNN was the most stable, with the MSE of 0.0114. There were certain fluctuations during the fitting process of SVM. The R^2 of the multiple linear regression was just 0.87, indicating that it did not fit well. In summary, the effective trend of milling parameters on the surface roughness of Scots pine during the milling process was similar to multiple nonlinear regression, and NN was an effective method for prediction.

CONCLUSIONS

In this paper, multiple milling settings for straight tooth milling of Scots pine were specified. The study's limitations were that only the rake angle, spindle speed, and milling depth were used to assess the workpiece's surface quality. Other tool parameters' effects on the workpiece were not taken into account. After theoretical analysis, four types of computational approach were employed to predict surface roughness by considering the above parameters, with the following conclusions:

1. The theoretical analysis based on the main effects revealed that all the milling parameters had the main influence on the surface roughness of Scots pine. The workpiece surface roughness rose as the rake angle and milling depth increased, but they decreased as spindle speed increased.
2. Good concurrence was found between the milling force and surface roughness. They both increased with the increase of the milling depth but were negatively correlated with the spindle speed and tool rake angle.
3. The surface roughness results from the models (BPNN, RBFNN, SVM and multiple linear regression) illustrated that the predictive accuracy of the BPNN was relatively minimal, with the MAP of 1.02%.

4. NN had the best performance of the four computational approaches, with an R^2 of 0.98. In particular, the fitting process of BPNN was the most stable, with a MSE of 0.0114. By using the model of SVM, the R^2 and MSE were not very good, compared with NN model. The surface roughness prediction model of straight tooth milling Scots pine was not suitable for linear regression analysis, which R^2 was just 0.87.

Funding

This study was funded by the Efficient Processing Technology for Unusual and Low-grade Wood (supported by *Science and Technology*) (Grant No. 011020267).

Availability of Data and Materials

The datasets generated and analyzed during the current study are available from the corresponding author on request.

Ethics Approval

No studies involving humans or animals are included in this article.

Competing Interests

The authors declare that they have no conflict of interest.

REFERENCES CITED

Byrne, G., Dornfeld, D., and Denkena B. (2003). "Advancing cutting technology," *CIRP Annals* 52(2), 483-507. DOI: 10.1016/S0007-8506(07)60200-5

Chen, D., Satran, A., and Ziebenberg, A. (2012). "Tangential cutting insert and milling cutter," U. S. Patent No. 20120195700A1.

Cho, S., Asfour, S., Onar, A., and Kaundinya, N. (2005). "Tool breakage detection using support vector machine learning in a milling process," *International Journal of Machine Tools and Manufacture*, 45(3), 241-249. DOI: 10.1016/j.ijmachtools.2004.08.016

Cui, K., and Xiang, J. (2018). "Research on prediction model of geotechnical parameters based on BP neural network," *Neural Computing and Applications* 31(14), 8205 - 8215. DOI: 10.1007/s00521-018-3902-6

Darmawan, W., Tanaka, C., Usuki, H., and Ohtani, T. (2001). "Performance of coated carbide tools when grooving wood-based materials: Effect of work materials and coating materials on the wear resistance of coated carbide tools," *Journal of Wood Science* 47(2), 94-101. DOI: 10.1007/BF00780556

Dong, W., Guo, X., Hu, Y., Wang, J., and Tian, G. (2021). "Discrete wavelet transformation and genetic algorithm – Back propagation neural network applied in monitoring woodworking tool wear conditions in the milling operation spindle power signals," *BioResources* 16(2), 2369-2384. DOI: 10.15376/biores.16.2.2369-2384

Eyma, F., Méausoone, P., and Martin, P. (2004). "Strains and cutting forces involved in the solid wood rotating cutting process," *Journal of Materials Processing Tech* 148(2), 220-225. DOI: 10.1016/S0924-0136(03)00880-X

Gharagheizi, F. (2007). "Qspr analysis for intrinsic viscosity of polymer solutions by means of ga-mlr and rbfnn," *Computational Materials Science* 40(1), 159-167. DOI: 10.1016/j.commatsci.2006.11.010

Guillen, A., Pomares, H., Gonzalez, J., Rojas, I., Valenzuela, O., and Prieto, B. (2009). "Parallel multiobjective memetic rbfnns design and feature selection for function approximation problems," *Neurocomputing* 72(16-18), 3541-3555.

Guo, X., Ekevad, M., Grönlund, A., Marklund, B., and Cao, P. (2014). "Tool wear and machined surface roughness during wood flour/polyethylene composite peripheral up-milling using cemented tungsten carbide tools," *BioResources* 9(3), 3779-3791. DOI: 10.15376/biores.9.3.3779-3791

Guo, X., Li, R., Cao, P., Ekevad, M., Cristovao, L., Marklund, B., and Gronlund, A. (2015). "Effect of average chip thickness and cutting speed on cutting forces and surface roughness during peripheral up milling of wood flour/polyvinyl chloride composite," *Wood Research* 60(1), 147-156.

Guo, X., Wang, J., Buck, D., Zhu, Z., Ekevad, M. (2021). "Cutting forces and cutting quality in the up-milling of solid wood using ceramic cutting tools," *The International Journal of Advanced Manufacturing Technology* 114(5), 1575-1584. DOI: 10.1007/s00170-021-06991-x

Guo, X., Wang, J., Buck, D., Zhu, Z., and Guo, Y. (2021). "Machinability of wood fiber/polyethylene composite during orthogonal cutting," *Wood Science and Technology* 55(2), 1-14. DOI: 10.1007/s00226-020-01256-4

Keturakis, G., and Bendikiene, R. (2016). "Influence of chemical composition of steels on the wood milling knives wear," in: *18th International Conference - School Advanced Materials and Technologies 2016*, Palanga, Lithuania, p. 139.

Li, W., F Pan, and Cao, W. (2013). "Study on feature selection and identification method of tool wear states based on svm," *International Journal on Smart Sensing and Intelligent Systems, 6*(N°2), 448-465. DOI: 10.21307/ijssis-2017-549

Liu, C., He, Y., Wang, Y., Li, Y., and Wang, Y. (2020). "Effects of process parameters on cutting temperature in dry machining of ball screw," *ISA Transactions*, 101. DOI: https://doi.org/10.1016/j.isatra.2020.01.031

Liu, S., Jin, S., Zhang, X., Chen, K., Wang, L., and Zhao, H. (2018). "Optimization of 3D surface roughness induced by milling operation for adhesive-sealing," *Procedia CIRP* 71, 279-284. DOI: 10.1016/j.procir.2018.05.011

Luo, J. (2007). "NC milling cutter selection and cutting amount determination," *Mechanical Management and Development* 2007(S1), 87-90. DOI: 10.16525/j.cnki.cn14-1134/th.2007.s1.043

MalkoçoğLu, A. (2007). "Machining properties and surface roughness of various wood species planed in different conditions," *Building & Environment* 42(7), 2562-2567. DOI: 10.1016/j.buildenv.2006.08.028

Ma, L., Li, C., Chen, J., Li, W., Tan, Y., Wang, C., and Zhou, Y. (2016). "Prediction model and simulation of cutting force in turning hard-brittle materials," *International Journal of Advanced Manufacturing Technology* 91(1-4), 165-174. DOI: 10.1007/s00170-016-9642-9

Rudawska, A., Reszka, M., Warda, T., Miturska, I., Szabelski, J., Stančeková, D., and Skoczylas, A. (2016). "Milling as a method of surface pre-treatment of steel for adhesive bonding," *Journal of Adhesion Science and Technology* 30(23), 1-18. DOI: 10.1080/01694243.2016.1191585

Sogutlu, C., Kaya, M., and Imirzi, H. O. (2017). "Effect of cutter types, spindle speed and

feed rate on the surface quality in cnc milling," in: *The XXVIII International Conference Research for Furniture Industry*, Poznan, Poland, 21-22 September 2017.

Sofuoğlu, M. A. (2019). "Prediction of stable depth of cuts in turning and milling operations: A new probabilistic approach," *Journal of the Brazilian Society of Mechanical Sciences and Engineering* 41(5), article no. 206. DOI: 10.1007/s40430-019-1706-y

Sun, Y., J Xu, Qiang, H., Chen, and Lin, G. B. (2019). "Adaptive sliding mode control of maglev system based on rbf neural network minimum parameter learning method," *Measurement*, 141. DOI: 10.1016/j.measurement.2019.03.006

Tiryaki, S., Malkoçoğlu, A., and Ozsahin, S. (2014). "Using artificial neural networks for modeling surface roughness of wood in machining process," *Construction and Building Materials* 66, 329-335. DOI: 10.1016/j.conbuildmat.2014.05.098

Tu, K., Wang, X., Kong, L., and Guan, H. (2018). "Facile preparation of mechanically durable, self-healing and multifunctional superhydrophobic surfaces on solid wood," *Materials and Design* 140(FEB.), 30-36. DOI: 10.1016/j.matdes.2017.11.029

Umut, K. and Erhan, B. (2018). "Investigating effects of milling conditions on cutting temperatures through analytical and experimental methods," *Journal of Materials Processing Technology*, 262, S0924013618303200-. DOI: 10.1016/j.jmatprotec.2018.07.024

Valarmathi, T. N., Palanikumar, K., and Sekar, S. (2015). "Modeling of surface roughness in drilling of MDF panels," *Applied Mechanics and Materials* 766-767, 831-836. DOI: 10.4028/www.scientific.net/AMM.766-767.831

Vančo, M., Mazán, A., Barcík, S., Rajko, L., Koleda, P., Vyhnáliková, Z., and Safin, R. R. (2017). "Impact of selected technological, technical, and material factors on the quality of machined surface at face milling of thermally modified pine wood," *BioResources* 12(3), 5140-5154. DOI: 10.15376/biores.12.3.5140-5154

Wang, D., and Chen, J. (2005). "Prediction of cutting force using BP artificial neural network," *Journal of Dalian University of Technology* 45(6), 814-818.

Wang, S. Y., Xing, A. I., Zhao, J., Li, L. Z. and Liu, Z. W. (2006). "Milling force prediction model for high-speed end milling 3cr2mo steel," *Journal of Shandong University*. DOI: 10.1016/S1003-6326(06)60027-7

Wang, L. Y., and Huang, H. H. (2010). "Milling force of plastic mold parts in high speed hard milling based on BP neural network," *Journal of Central South University (Science and Technology)* 41(6), 2218-2223.

Yue, C., Huang, C., Liu, X., Hao, S., and Liu, J. (2017). "3D FEM simulation of milling force in corner machining process," *Chinese Journal of Mechanical Engineering* 30(2), 286-293. DOI: 10.1007/s10033-017-0088-2

Zhang, L., Wang, F., Sun, T., and Xu, B. (2018). "A constrained optimization method based on BP neural network," *Neural Computing and Applications* 29(2), 413-421. DOI: 10.1007/s00521-016-2455-9

Zhang, M., Liu, Y., and Yang, Z. (2015). "Correlation of near infrared spectroscopy measurements with the surface roughness of wood," *BioResources* 10(4), 6953-6960. DOI: 10.15376/biores.10.4.6953-6960

Zhao, H., Feng, B., Dong, X., and Zhenhua, W. U. (2008). "Optimization choice of cutting parameter based on improved BP neural network," *Machine Tool & Hydraulics* 36(5), 213-215.

Zheng, M. L., Jiang, B., Liu, J., and He, C. Y. (2008). "Research on dynamic cutting performance of high speed face milling cutter," *Key Engineering Materials* 375-376,

663-666. DOI: 10.4028/www.scientific.net/KEM.375-376.663

Zhong, Z. W., Hiziroglu, S., and Chan, C. T. M. (2013). "Measurement of the surface roughness of wood based materials used in furniture manufacture," *Measurement* 46(4), 1482-1487. DOI: 10.1016/j.measurement.2012.11.041

Zhu, Z., Buck, D., Guo, X., Ekevad, M., Cao, P., and Wu, Z. (2018). "Machinability investigation in turning of high density fiberboard," *PLoS ONE* 13(9), article ID e0203838. DOI: 10.1371/journal.pone.0203838

Article submitted: November 24, 2021; Peer review completed: December 19, 2021; Revised version received and accepted: January 30, 2022; Published: February 4, 2022.
DOI: 10.15376/biores.17.2.2003-2019